

# BEAM ARRIVAL-TIME AND POSITION MEASUREMENTS USING ELECTRO-OPTICAL SAMPLING OF PICKUP SIGNALS

K. Hacker,\* DESY, Hamburg, Germany

## Abstract

By using magnetic chicane bunch compressors, high-gain free-electron lasers are capable of generating femtosecond electron bunches with peak currents in the kilo-ampere range. For accurate control of the longitudinal dynamics during this compression process, high-precision beam energy and arrival-time monitors are required. Here we present an electro-optical detection scheme that uses the signal of a beam pickup to modulate the intensity of a femtosecond laser pulse train. By detecting the energies of the laser pulses, the arrival-time of the pickup signal can be deduced. Depending on the choice of the beam pickup, this technique allows for high-resolution beam position measurements inside of magnetic chicanes and/or for femtosecond-resolution bunch arrival-time measurements. In first prototypes we realized a beam position monitor with a resolution of 3  $\mu\text{m}$  (rms) over a many-centimeter dynamic range and a bunch arrival-time monitor with a resolution of 6 fs (rms) relative to a pulsed optical reference signal.

## INTRODUCTION

A beam arrival-time stability of  $\sim 30$  fs rms ( $\sim 10$   $\mu\text{m}$  at  $v=c$ ) is desired for pump-probe experiments and is mandatory for laser-based electron beam manipulation at FLASH and the European XFEL [1]. Arrival-time jitter in these FELs is primarily created by energy-dependent path-length changes in the magnetic bunch compressor chicanes. The first bunch compressor of the FLASH linac is shown below in Fig. 1 with the orbit for an  $R_{16} = 350$  mm and  $R_{56} = 620$  ps plotted in green. The locations of beam pickups used for measuring the beam arrival-time and position are indicated with yellow stars.

With the accelerating RF gradient stability of  $10^{-4}$  at FLASH, the transverse position jitter in the dispersive section of the first chicane becomes 35  $\mu\text{m}$  and the longitudinal position jitter becomes 18  $\mu\text{m}$ . A beam-based monitor for an RF gradient feedback system should be able to measure the beam energy by a factor of three better than the desired energy stability of  $5 \cdot 10^{-5}$  and this means that the resolution for a beam position measurement in the chicane must be better than 6  $\mu\text{m}$  and a longitudinal time-of-flight path-length measurement should resolve 3  $\mu\text{m}$ . Each measurement must have a many-centimeter range in order to accommodate different machine configurations.

Devices meeting these requirements were made possible through a technique that involves sampling the zero-crossings of electrical beam pickup signals with

short laser pulses. The 20-200 fs pulses from a mode-locked erbium-doped fiber laser are sent over actively length-stabilized fiber links to distant end-stations, whereupon the amplitudes of the laser pulses are modulated by the amplitudes of the beam pickup signals with a commercially available electro-optical modulator. The modulated laser pulses then impinge upon a photodetector, and the amplitude of the photo-detector signal is recorded with an ADC, which is clocked with a signal generated from the very same laser pulse train. These sorts of measurements are vital for the pulsed optical synchronization system at FLASH and the beam-based energy and timing feedbacks upon which it relies.

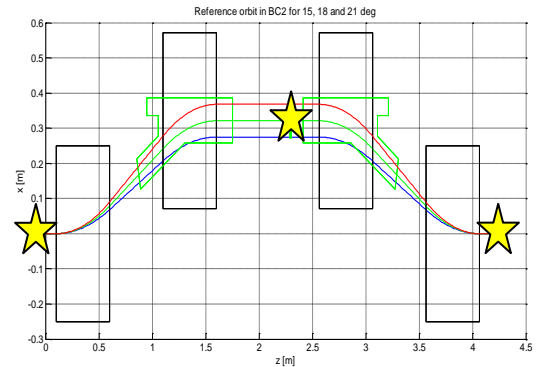


Figure 1: First magnetic bunch compressor chicane at FLASH. Dipoles are drawn in black, the vacuum chamber is drawn in green, and the locations of pickups for beam arrival-time and position measurements are indicated by yellow stars. Higher- and lower-energy particle beams travel a longer or shorter path-length through the chicane, affecting the beam arrival time after the chicane.

This technique has been verified with two types of pickups. Using two sets of broadband, button-like pickups separated by 60 m in a drift section, two independent measurements of the beam arrival-time were conducted, verifying the 6 fs (rms) resolution of the method [2,3]. In another experiment, involving a transversely mounted stripline pickup in the dispersive section of the chicane [4,5], 3  $\mu\text{m}$  (rms) beam position resolution over a 10 cm range was achieved and cross-checked against a synchrotron light-based BPM [6,7]. The arrival-time measurements conducted with this stripline pickup were also cross-checked with a beam arrival-time measurement conducted upstream of the chicane with button-like pickups [7]. A description of how these measurements are locked to an RF reference follows [7].

\* kirsten.hacker@desy.de

## PULSED OPTICAL SYNCHRONIZATION

The pulsed optical synchronization system at FLASH relies on the delivery of short laser pulses with a stable repetition rate to remote end-stations [8]. This must be done with a high level of phase stability. This is accomplished through feedback loops, which stabilize the optical lengths of the fibers over which the pulses are sent. Such a scheme is shown below in Fig. 2. The arrival-times of the master laser oscillator pulses relative to the pulses returning to the device can be measured through optical cross-correlation or through an RF method. The optical method can get a best-case resolution of less than a femtosecond (rms) [9], but is much more expensive, unstable, and complicated than the RF method which can get a best-case resolution of 5 fs (rms) [10].

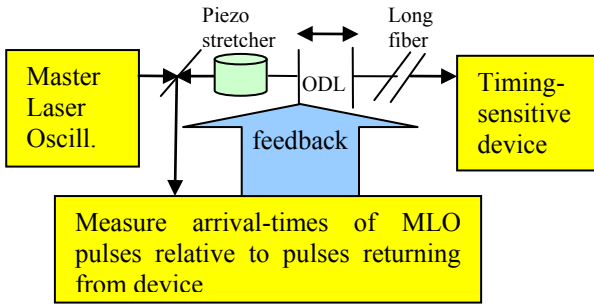


Figure 2: The optical length of a fiber link is stabilized so that the pulses from the master laser oscillator arrive at a stable time at a timing sensitive device.

The timing-sensitive device in Fig. 2 can be a laser, a beam arrival-time or position monitor (BAM or BPM), or a (yet-unproven) laser-to-RF conversion unit. Lasers are locked together using optical cross correlation and the beam arrival-time and position monitors utilize the pulsed signals from beam pickups to modulate the amplitudes of the laser pulses in a compact, commercially available device called a Mach-Zehnder Electro-Optical Modulator (EOM) shown in Fig. 3.

In Fig. 3, the laser pulses travel through LiNbO<sub>3</sub> crystal. When the crystal is under the influence of an electric field it becomes birefringent and causes a phase shift of the light that is transmitted. The electric field from the pickup signal is applied to the crystal with opposite polarities so that the phase velocity of the laser pulses increases in one arm and decreases in the other arm. When the laser pulses are recombined, they interfere constructively or destructively in proportion to the amplitude of the applied electric field.

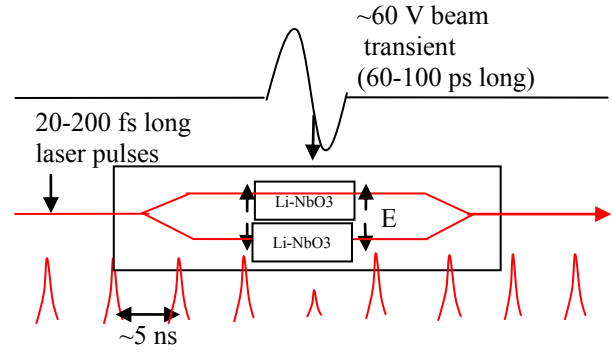


Figure 3: Mach-Zehnder Electro-Optical Modulator (EOM) used to modulate laser amplitude with zero-crossing of beam pickup signal.

The amplitudes of the modulated laser pulses are converted into electrical signals with photodetectors. The amplitudes of the electrical pulses from the photodetectors are sampled with an ADC, which is clocked with a signal generated from another photodetector signal (Fig. 4).

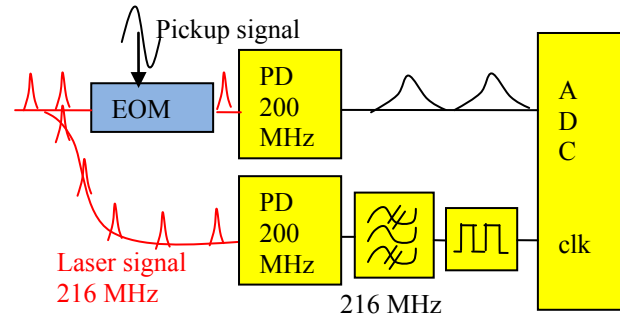


Figure 4: The arrival-time of a pickup signal is measured with by using the zero-crossing of a beam pickup signal to modulate the amplitude of a laser pulse in an electro-optical modulator (EOM). The laser pulse amplitudes are detected with a photodetector and an ADC that is clocked with a signal generated from the laser pulse train.

The measurements of the pickup signal's phase are calibrated by using an optical delay line to vary the arrival-time of the laser pulses at the EOM. With the appropriate laser timing, this enables a scan about the zero-crossing of the pickup signal and a measurement of the signal's slope in terms of the modulation of the laser pulse amplitude (Fig. 5).

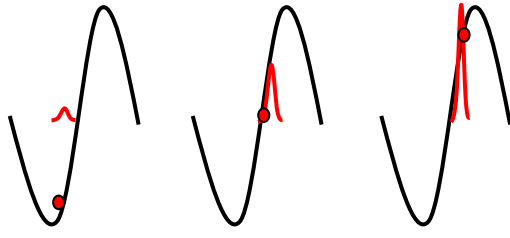


Figure 5: Scanning the arrival-time of the laser pulse (red) over the pickup pulse (black) in order to determine a calibration constant for the measurement of the arrival-time of the pickup pulse.

To give an idea of the way that the amplitude of the laser pulse changes when its arrival-time is scanned relative to the arrival-time of a pickup signal, scans for four pickup signals are plotted below in Fig. 6. The red and pink pickup signals are attenuated and an RF limiter is used with the blue and black pickup signals. When the signal is attenuated, the dynamic range increases and the resolution decreases. The signals with the larger dynamic range are used to deliver commands to an optical delay line and keep the signals with the higher resolution in range.

The black and blue signals look rather strange because of over-rotation in the EOMs. When a pickup signal amplitude exceeds the linear range of the EOM, the EOM does not just saturate and deliver a flat response; the polarization in the EOM continues to change. This is why, when the amplitude of the pickup signal is large, the black and blue signals seen in the scan shown in Fig. 6 invert.

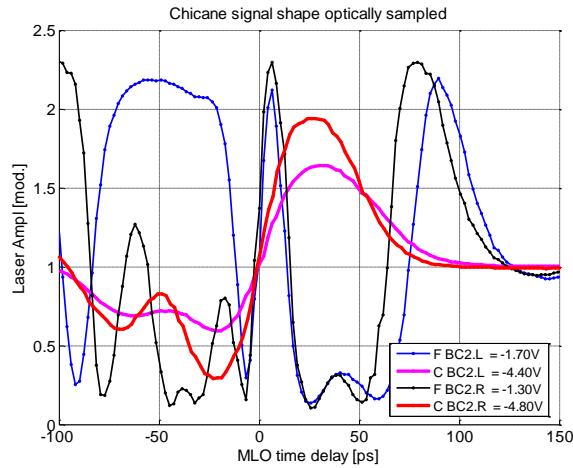


Figure 6: Laser amplitude changes as the laser arrival-time is shifted relative to four different pickup signals. The red and pink pickup signals are attenuated and an RF limiter is used with the blue and black pickup signals.

When the phase of the laser is coincident with the zero-crossing of the pickup, this optical sampling method allows for high-precision measurements of the phase of the pickup signal. The resolution of the method is determined by the accuracy with which the laser pulse amplitude can be detected and the steepness of the slope of the electrical signal. In the 6 fs resolution measurements presented in [2,3,7], the signal slope steepness was typically around 1 V/ps and the accuracy with which the laser pulses could be detected was about 0.1% of a 1V ADC input.

## BEAM ARRIVAL TIME WITH BUTTONS

To generate these steep signal slopes for beam arrival-time measurements in straight sections, button-like pickups with a broadband output spectrum are used (Fig. 7). The vacuum feedthroughs used were type-N, so that the button size could be large without any steps in the coaxial line diameter. The signals from opposite buttons are combined in order to reduce the sensitivity of the phase measurement to changes in signal amplitude resulting from beam position changes. An RF limiter prevents damage to the EOM from large voltages resulting from beam spray.

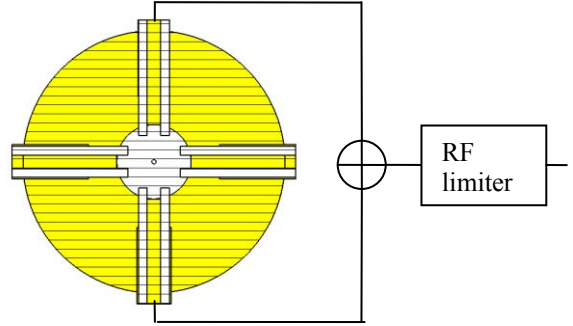


Figure 7: Cross section of broad-band button-like pickup for electro-optical sampling scheme. The signals from opposite sides are combined in order to reduce changes in amplitude that occur as a result of beam position changes. The RF limiter prevents damage to the EOM from large voltages resulting from beam spray [4,5].

Using two of these pickup assemblies, separated by 60 meters in a drift section, two cross-correlation-based, length-stabilized fiber links, and two EOM-based front-ends, the accuracy of the beam arrival-time measurement relative to the pulsed optical synchronization system reference was verified. Over short time scales, a difference of 9 fs (rms) between the two measurements was observed, implying that the measurement has a resolution of 6 fs (rms) [2,3]. Over longer time scales, the measurements differed by as much as 30 fs, with a large part of this discrepancy resulting from changes in the length of the long tail of the in-homogeneously compressed bunch. With homogenous compression, the influence of longitudinal bunch shape changes is expected to be smaller [3].

Some of the 30 fs of long-term measurement drift could also be attributed to drifts of the temperatures of the fibers in the EOM front ends. Each meter of fiber will drift by 60 fs per degree C, and there are up to two meters of fiber in each EOM front-end that are not stabilized by the fiber link stabilization feedback. This is why, in subsequent versions of the EOM front-end [6,7], the chassis was actively thermally stabilized to within 0.03° C, leaving a maximum thermal drift contribution for each front-end of less than 2 fs.

## BEAM ARRIVAL-TIME AND POSITION WITH PERPENDICULAR STRIPLINES

If a stripline pickup is mounted perpendicularly to the beam direction, as shown in Fig. 8, short electrical pulses will travel to the left and right sides of the pickup. If the arrival-times of these pulses are measured using the optical technique described previously, the beam position and arrival-time can be derived with

$$\text{beam\_position} = \frac{c}{2} \cdot \left( \text{arrival\_left} - \text{arrival\_right} \right)$$

and

$$\text{beam\_arrival} = \frac{1}{2} \cdot \left( \text{arrival\_left} + \text{arrival\_right} \right)$$

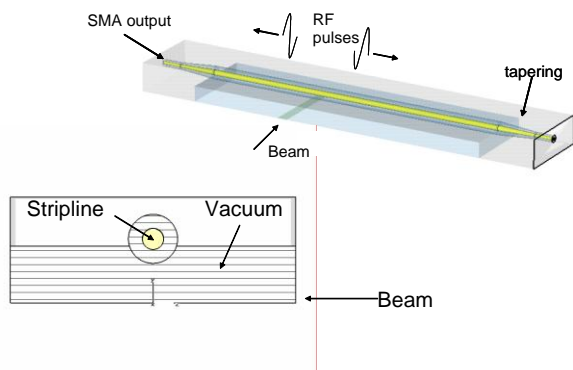


Figure 8: Top half of the perpendicularly mounted stripline BPM pickup. The pickup is suspended in a coaxially shaped channel, open to the vacuum chamber below. It is tapered to an SMA vacuum feed-through [4,5].

When the beam energy is changed, the beam position in the chicane will change in a predictable way. Measurements of the beam position, done by measuring the difference between the arrival-times of the zero-crossings of the pickup signals on an oscilloscope, are shown in Fig. 9 as a function of beam energy changes. Good agreement is observed over the full range of the pickup.

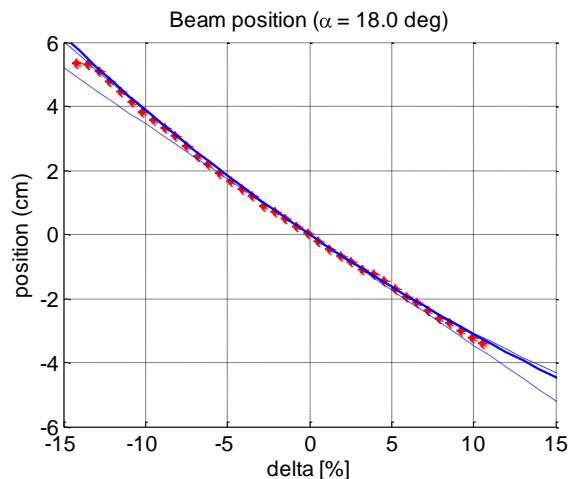


Figure 9: The beam position changes expected for a given energy change are plotted in blue for higher order dispersion terms. The measured position changes are plotted as red stars. This means that the pickup pulses from the transversely mounted stripline behave as expected when the beam position is changed over the full width of the vacuum chamber [5,7].

The signal slope remained steep when the energy spread and corresponding position spread were increased. The slope of the signal for different accelerating phases is plotted below in Fig. 10. Increasingly negative phases correspond to increasingly wider beams. This means that the pickup will function appropriately for wide beams.

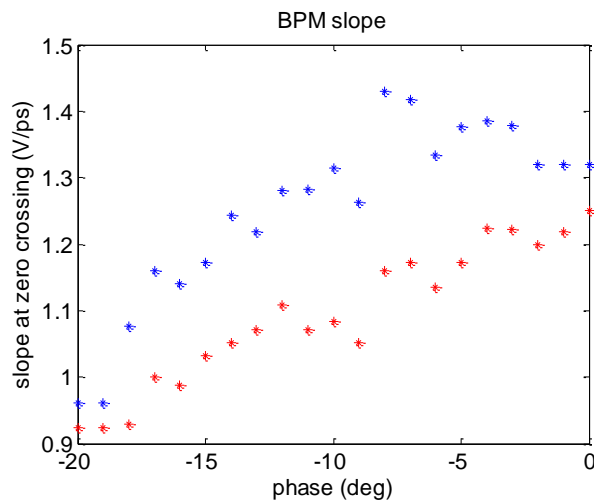


Figure 10: The slope of the pickup signal's zero crossing for different accelerating phases. Increasingly negative phases correspond to increasingly wider beams. This means that the pickup will function appropriately for centimeter wide beams [5,7].

A schematic for the optical front end for the transversely mounted stripline BPM/BAM is shown below in Fig. 11. The reference laser signal is tapped-off from a nearby length-stabilized end-point, the polarization of the signal is adjusted, the signal is amplified up to 200 mW with 4  $\mu\text{m}$  gain fiber pumped from both ends, and the arrival-time at each EOM is adjusted with Optical Delay Lines (ODLs). Fiber lengths and power levels are also described in the figure.

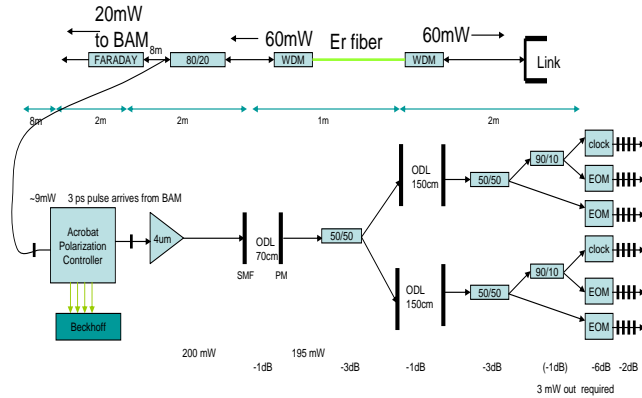


Figure 11: Schematic of optical beam arrival/position measurement front-end. An 8 m long, thermally insensitive patch-cord connects a nearby length-stabilized fiber link to the BPM chassis, whereupon the polarization is adjusted and the signal is amplified to 200 mW. The arrival-times of the laser pulses at 4 EOMs are adjusted with ODLs [5, 6].

The inside of the front-end is depicted in a top-view and a side-view in Fig. 12. In the top-view, the polarization controller is labelled with PC, the four EOMs are shown in the center, preceded by several splitters. The ODL on the left moves whenever the beam arrival-time changes, and the ODL on the right moves whenever the beam position changes. A linear encoder is mounted to the ODL on the right in order to provide an absolute position reference.

In the side-view, one of the Peltier elements used in the active thermal stabilization system is depicted in pink. Neoprene insulation is depicted in green and the surfaces of the chassis are depicted in turquoise. Heat from the plate upon which the EOMs and fibers rest is transferred to the outside of the chassis which is cooled with a fan. Stability of 0.03 degrees C has been achieved with this chassis installed in the tunnel.

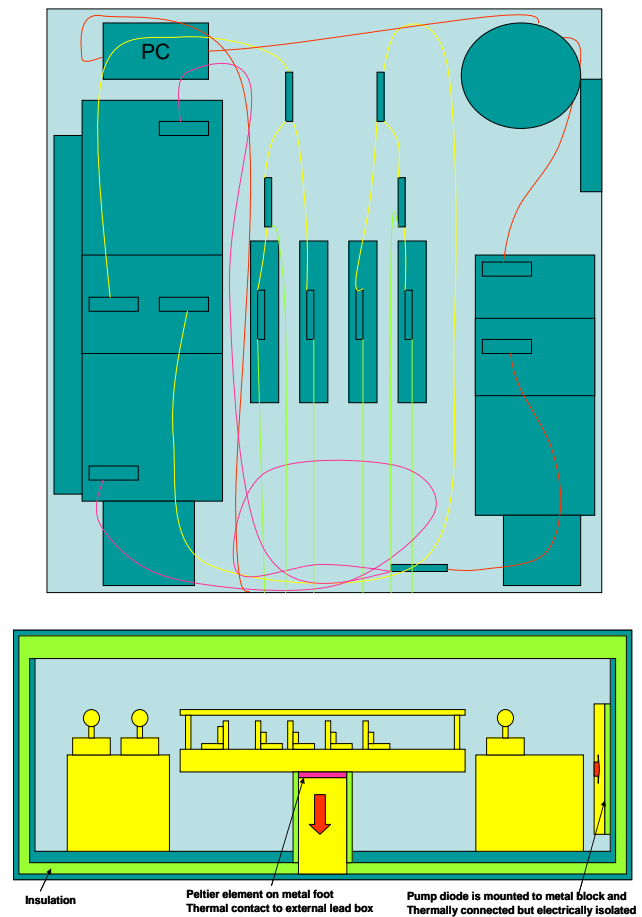


Figure 12: Physical layout of front-end chassis: (*upper*) top view with fiber routing and (*lower*) side view with thermal concept. The EOMs are depicted in the center and the optical delay lines (ODLs) are on the right and left sides of the chassis. The temperature of the plate upon which the EOMs and fibers rest is stabilized by pumping heat from the plate to the outside of the chassis, which is cooled by a fan [6, 7].

The setup described above was used in the measurements of the signals from the transversely mounted stripline pickup [7]. A similar setup with fewer EOMs is used in recent button-based beam-arrival-time measurements [12]. The older version of the optical pickup sampling front-end [3] had the disadvantages that the optical delay-stages had a low mean-time-to-failure and the chassis was not thermally stabilized.



Once the measurement set-up is commissioned, the first step is to verify the calibration of the measurement with a beam-based reference. If the calibrations of the pickup signal arrival-time measurements from both sides of the transversely mounted pickup are correct, then, when the energy of the beam is changed, the ratio of the change of the arrival-times of the signals will be equal to  $(R_{56}/2+R_{16})/(R_{56}/2-R_{16})$ . Fig. 13 verifies that the calibrations do satisfy this requirement, even though the beam jitter was large, requiring averaging over multiple shots.

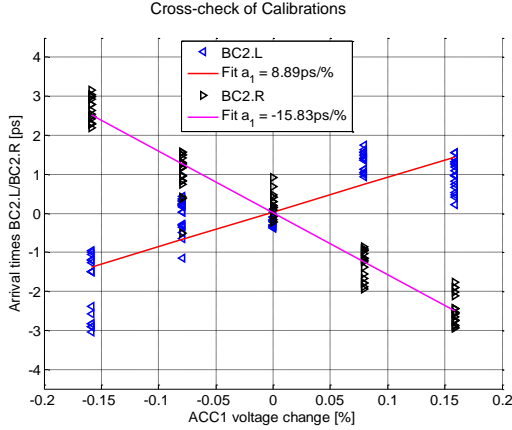


Figure 13: Verification of the calibrations of the pulse arrival-time measurements for the left and right sides of the pickup.  $BC2.L/BC2.R = (R_{56}/2+R_{16})/(R_{56}/2-R_{16})$ . [7].

When the transversely mounted stripline pickup is installed in a dispersive section of a chicane, it is possible to use the beam position and arrival-time information to calculate energy changes of the beam according to

$$\frac{\Delta E}{E} = R_{16} \cdot \Delta x_{chicane}.$$

In Fig. 14, the energy changes measured by the pickup are plotted as a function of the bunch number in the bunch train. Because the dynamic range of the measurement is small when the resolution is high, only the central portion of the bunch train is within the range of the measurement and agrees with the 0.3% amplitude change made in the set-point of the accelerator module.

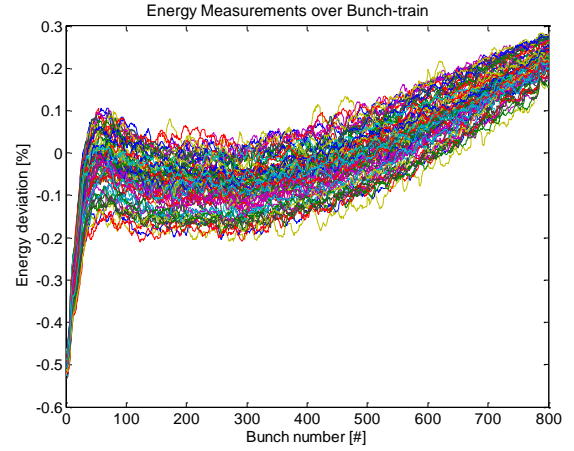


Figure 14: Changes in beam energy measured with the transversely mounted stripline monitor in the dispersive section of the bunch compressor. Because the dynamic range of the measurement is limited, only the central portion of the bunch train agrees with amplitude changes made in the set-point of the accelerator module [7].

The transversely mounted stripline pickup in a dispersive section can also measure arrival-time changes that occur prior to the dispersive section, using

$$t_{upstream} = \frac{R_{56}}{R_{16}} x - t_{chicane}.$$

The arrival-time upstream of the chicane is plotted in Fig. 15, as measured with the transversely-mounted stripline installed in the dispersive section of the chicane and with a button-like pickup installed upstream of the chicane. The dynamic range of the stripline measurement is exceeded near the end of the bunch train. The stripline measurement also suffered from buffer number problems, causing the measurement of the signal from the right side of the pickup to not always be from the same shot as the measurement from the left side of the pickup. Despite this problem, the 50 kHz ripple due to an RF gun oscillation is visible in both measurements, and slight adjustments to the calibration constants of each measurement can bring them into better agreement.

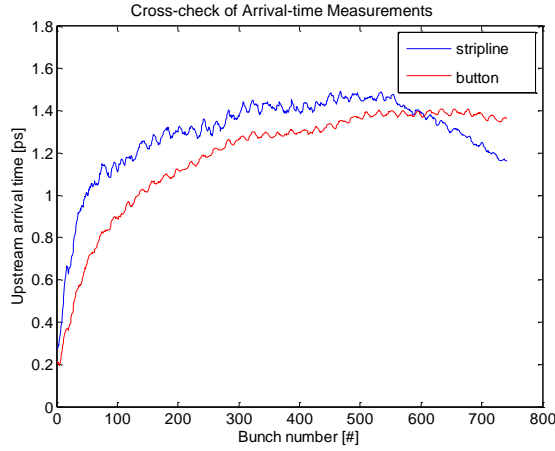


Figure 15: The beam arrival-time upstream of the chicane measured with a button pickup installed upstream of the chicane and with the stripline pickup installed in the chicane [7].

How the beam shape influences the two measurements will be actively studied in the future. In simulations, by comparing the stripline and button measurements, it should be possible to extract the beam width (energy spread) in the chicane when the beam length and height are smaller than its width (Fig. 16).

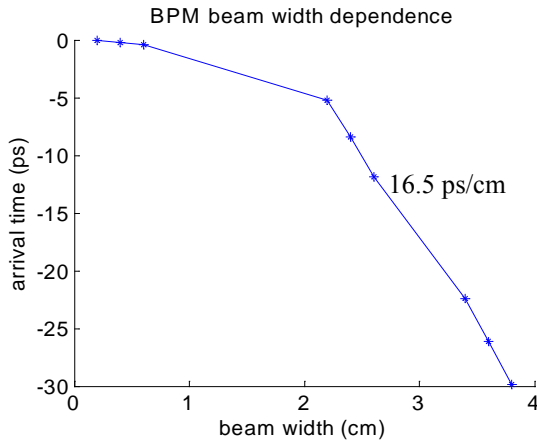


Figure 16: Simulation of the dependence of the arrival-time of a bunch at the transversely mounted stripline on the width of the bunch.

In simulations and measurements, the beam tilt also has a significant impact on the stripline measurements. By applying closed orbits bumps upstream of the chicane it is possible to control the tilt of the beam in the chicane. The tilt can be accurately measured with a synchrotron light monitor and the effect on the measurement of the beam position in the chicane with the transversely mounted stripline is plotted below in Fig. 17.

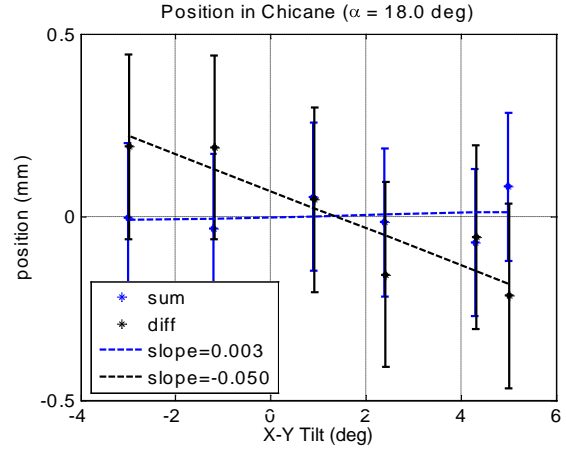


Figure 17: The position measured in the chicane as a function of the x-y tilt of the beam measured on a synchrotron light monitor. The beam width in this measurement was 50 mm (rms) [7].

While any y-z tilts can be removed by combining the signals from the top and bottom pickups, systematic errors that occur due to asymmetric distributions tilted in the x-z plane cannot be removed by any means. These errors can be as large as half a millimeter.

A final cross-check of the stripline beam position measurement can be provided by a synchrotron-light based BPM that uses two photo-multiplier tubes to determine the beam position. It is labelled PMT in Fig. 18, below.

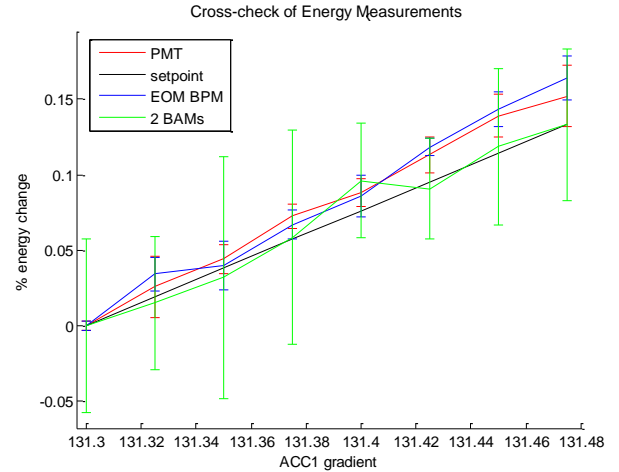


Figure 18: Changes in beam energy measured with a synchrotron light based BPM (PMT) are plotted in red, the transversely mounted stripline (EOM BPM) is plotted in blue, the setpoint of the accelerator section gradient (setpoint) is in black, and a measurement with two button pickup beam arrival-time monitors in a time-of-flight measurement (2 BAMs) is shown in green. The error bars on the 2 BAM measurement are large because a second accelerator section and bunch compressor were located between the first BAM and the second BAM [6, 7].

In Fig. 18, the gradient setpoint of the accelerator section was changed and the beam energy changes expected based on cavity regulation were plotted in black. The energy changes measured by the transversely mounted stripline are plotted in blue, the synchrotron light based measurements are in red, and the time-of-flight measurements done with two button pickup beam arrival-time monitors are shown in green. The error bars on the time-of-flight measurement are large because a second accelerator section and a bunch compressor were located between the first BAM and the second BAM [6,7]. When more BAMs are commissioned, this will not be the case and the time-of-flight measurement is expected to have an resolution that is only a factor-of-two worse than that of the transversely mounted stripline.

The main limitation of the BAM/BPM resolution is not, however, presently given by the pickup bandwidth or the ratio of the  $R_{56}$  to the  $R_{16}$ . It is determined by the stability of the beam arrival-time and position. When the beam is unstable, the  $\sim$ millimeter dynamic range of the monitors must be increased by attenuating the pickup signals. This increase in dynamic range comes at the expense of resolution.

## MASTER LASER OSCILLATOR RF LOCK

All of the beam arrival-time measurements quoted here have been relative to an optical reference. These would be useless measurements unless the master optical reference is locked to the master RF reference. While the master laser oscillator has excellent short-term phase stability ( $\sim 4$  fs (rms)), it has terrible long-term phase stability. If a source with a good short-term stability and a bad long-term stability is locked with a low-bandwidth to a source with a good long-term stability, the source with the good short-term stability will acquire the long-term stability of the device to which it is locked.

Stability is the goal when the phases of pulses produced by a Master Laser Oscillator (MLO) are measured relative to a Master RF Oscillator (MO) signal phase (Fig. 19) [11]. The measurements of this phase difference are used in a Digital Signal Processing (DSP) regulation loop to adjust the position of mirror in the MLO cavity, thereby adjusting the phase of the MLO.

In the phase measurement schematic shown in Fig. 19, the pulses from the MLO are impinged upon a 10 GHz photo-detector that resides directly within the laser housing. This is on the far left of the drawing, with laser signals drawn in red and electrical signal drawn in black. The photodetector output is sent, via a 6 meter long RF-cable, to a rack containing phase measurement RF electronics in a chassis that is temperature stabilized to within  $0.001^\circ\text{C}$  (rms).

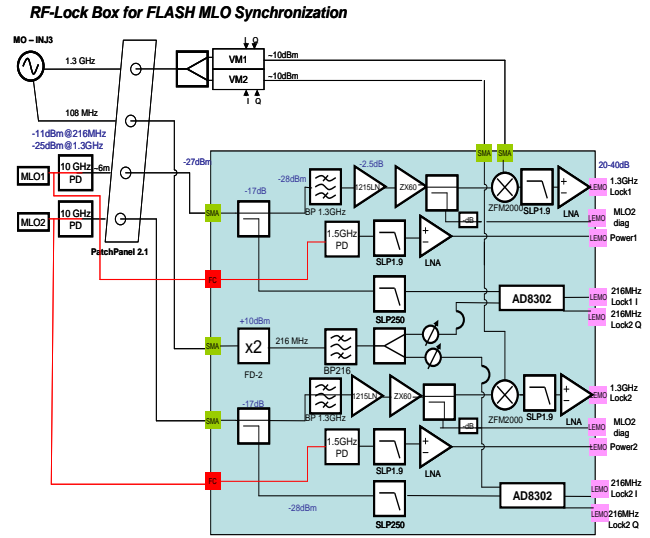


Figure 19: Schematic of MLO – MO phase measurements [11]. The pulses from the MLO (red) are impinged upon a 10 GHz photodetector that resides directly within the laser housing. The photodetector output (black) is sent, via a 6 meter long RF-cable, to a rack containing phase measurement RF electronics in a chassis (blue) that is temperature stabilized to within  $0.001^\circ\text{C}$  (rms) [11].

The circuit shown in Fig. 19 is designed to support two MLOs and two 1.3 GHz MLO-MO lock circuits. In the evaluation of the lock performance, one of the two identical circuits was used to lock the MLO to the MO and provide an in-loop measurement and the other was used for an out-of-loop measurement. In addition to the 1.3 GHz phase measurement circuits, a pair of AD8302 216 MHz phase and amplitude detection circuits are employed to provide a coarse reference against which bucket jumps of the PLL can be diagnosed. The MO reference is shifted with a vector modulator board that is controlled with a DAC. This functionality is used, for checks of the calibration of the circuit.

Using input signals from a signal generator instead of from the filtered photodetector signals, the noise contribution of the phase measurement circuit can be evaluated. In Fig. 20, the noise contribution of the phase measurement is less than 6.5 fs, with a majority of the noise coming from frequencies which are above the bandwidth of the PLL. These frequencies will not affect the measurement. The main noise source is the photodetector signal, which contributed  $\sim 15$  fs of phase noise.



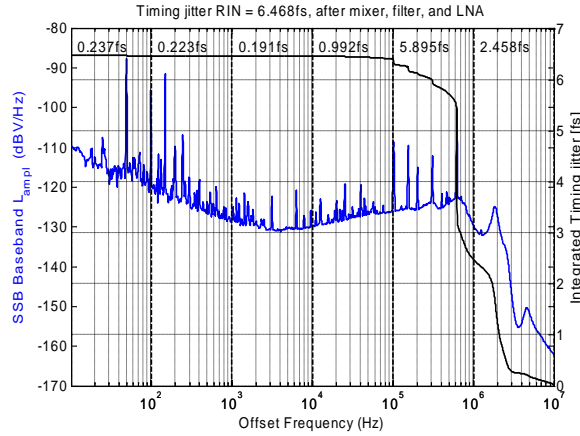


Figure 20: Noise contribution of phase measurement: baseband noise of the mixer output with amplification. Although high frequency noise is added through the amplifier, frequencies above 10 kHz are later filtered out in the regulation. The K-phi was 350 mV/deg [11].

Using input signals from a signal generator instead of from the filtered photodetector signals, the long-term drift performance of the phase measurement was below 5 fs in an undisturbed, climatized room with active temperature control within the chassis, but it jumped by 15 fs when people entered the room. Without the active temperature stabilization, the circuit drifts by 30 fs in an undisturbed, climatized room and by picoseconds when people are working in the room.

When the filtered photo-detector signals were used and the DSP regulation loop was closed, an out-of-loop drift of 77 fs was measured over an undisturbed 24-hour period (Fig. 21 (top)). The out-of-loop drift was dominated by the effects of laser amplitude drift (Fig. 21 (top)). Because the active thermal stabilization was off during this measurement, 30 fs of drift should be expected due to thermal drift. Using active stabilization of the laser amplitude and active stabilization of the phase measurement circuit temperature, the main drift sources can be overcome, leaving a MLO-MO phase lock that can be made stable on the 10 fs level [11].

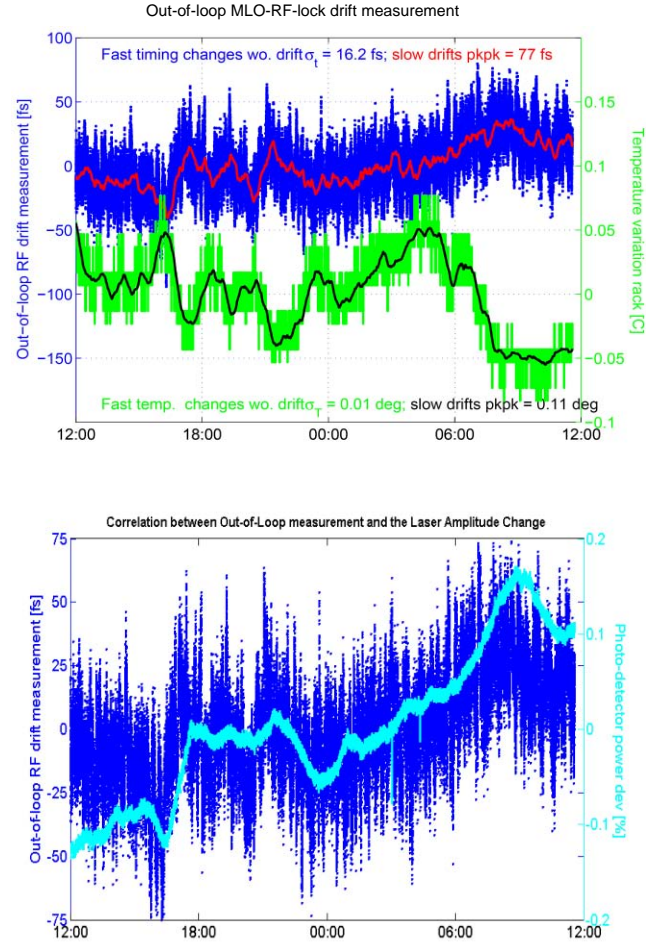


Figure 21: Laser amplitude drift (bottom) can account for 50 fs of the out-of-loop drift (top) [11].

## CONCLUSIONS

- A compact electro-optical technique makes 6 fs resolution pickup signal phase measurements possible as part of a pulsed optical synchronization system.
- 6 fs resolution phase measurements enable high resolution measurements of the beam arrival-time, energy, and position.
- The optical reference against which these measurements are made is locked to a stable RF reference.

## REFERENCES

- [1] X-FEL Technical Design Report Sect. 4.8 2006.
- [2] F. Loehl et al, "High-precision Beam Arrival Monitor", DIPAC 07, Venice, May 2007.
- [3] F. Loehl, "Optical Synchronization System for FLASH", PhD Thesis, University of Hamburg, June 2008.
- [4] K. Hacker *et al.*, "Beam pick-up designs suited for an electro-optical sampling technique", FEL 2006 Conference, Berlin, Germany, 2006.
- [5] K. Hacker et al, "Large Horizontal Aperture BPM and Precision Arrival Pickup", DIPAC 07, Venice, May 2007.
- [6] K. Hacker et al, "Demonstration of a BPM with 5  $\mu\text{m}$  Resolution over a 10 cm Range", DIPAC 09, Liverpool, May 2009.
- [7] K. Hacker, "Measuring the Electron Beam Energy in a Magnetic Bunch Compressor", PhD Thesis, University of Hamburg, July 2010.
- [8] S. Schulz *et al.*, "All-optical synchronization of distributed laser systems at FLASH", PAC 2009 Conference, Vancouver, Canada, 4-9 May, 2009.
- [9] J. Kim et al., "Long-term femtosecond timing link stabilization using a single-crystal balanced cross correlator", Opt. Lett. (2007), no. 9, 1044-1046.
- [10] J. Zemella et al., "RF-based detector for measuring fiber length changes with sub-5 femtosecond long-term stability over 50 h", FEL 2009 Conference, Liverpool, England, 23-28 August 2009.
- [11] K. Hacker et al, "Master Laser Oscillator RF-Lock", DIPAC 09, Liverpool, May 2009.
- [12] M. Bock et al, "Time-of-flight Measurement using two Beam Arrival-time Monitors", DIPAC 09, Liverpool, May 2009.

## ACKNOWLEDGEMENTS

The transversely mounted stripline pickup idea came from Manfred Wendt and the electro-optical pickup signal sampling idea came from Holger Schlarb. The optical synchronization infrastructure at FLASH has been under development over the past five years by a growing group of people, without whom these measurements wouldn't exist: M. Bock, M. Felber, P. Gessler, F. Loehl, F. Ludwig, H. Schlarb, B. Schmidt, S. Schulz, J. Szewinski, A. Winter, and J. Zemella. Additional thanks go to the many technicians who contributed their time and expertise to the designs.